Deep Resources Engineering 3 (2026) 100232

Contents lists available at ScienceDirect

Deep Resources Engineering

journal homepage: www.keaipublishing.com/en/journals/deepre/

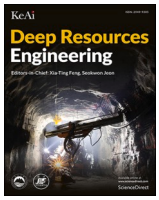

Full length article

Numerical and experimental studies of the natural mixing behavior between an uncemented paste backfill and dumped waste rock in stopes from laboratory toward field conditions. Part I: Calibration and validation of a numerical model

Yuyu Zhang [a], Li Li [a,*], Serge Ouellet [b], Louis-Philippe Gélinas [c]

[a] Research Institute of Mines and Environment (RIME UQAT-Polytechnique), Department of Civil, Geological and Mining Engineering, Polytechnique Montréal, C.P. 6079, Succursale Centre-Ville, Montréal, Québec H3C 3A7, Canada
[b] Agnico Eagle Mines Limited, 100, chemin du Lac Mourier, Malartic, Québec J0Y 1Z0, Canada
[c] Agnico Eagle Mines Limited, CSD, 10200, route de Preissac, Rouyn-Noranda, QC J0Y 1C0, Canada

ARTICLE INFO

Keywords:
Waste rocks
Paste backfill
Natural mixing behavior
Repose angle
Scalping method
Rolling resistance coefficient
Numerical modeling
Reliability

ABSTRACT

Underground mining operations generate large volumes of waste rock (WR). Transporting this material to the surface requires significant energy and incurs operational costs. As an alternative, WR can be directly dumped into stopes being filled with cemented paste backfill (CPB), reducing both costs and greenhouse gas emissions. However, inadequate dumping may lead to poor mixing between cohesionless WR and CPB, resulting in fill mass collapse during or after adjacent stope excavation. Understanding and quantifying the natural mixing between dumped WR and CPB is therefore critical; yet, such studies are scarce. A major challenge lies in replicating large-scale field behavior through limited laboratory-scale tests using scalped (truncated) WR samples. Numerical modeling becomes essential to capture size effects related to both stope and WR particle sizes. In this study, a discrete element method (DEM)-based numerical model was employed. It was first calibrated using repose angle tests on WR samples with varying maximum particle sizes (d_{max}), prepared using the scalping-down technique. All model parameters were determined through direct measurements, except for the rolling resistance coefficient (μ_r) between WR particles, which should be obtained through numerical calibration. Initially, it was assumed that the μ_r would vary with d_{max}, in line with the observed increase in repose angle with larger d_{max}. Surprisingly, calibration showed that μ_r was not very sensitive to changes in d_{max}, contradicting the experimental trend. Further investigation revealed that repose angle measurements are influenced by the quantity of material used; when sufficient WR mass is employed, the repose angle also becomes independent of d_{max}. This confirms that scalped samples can reliably represent in situ WR in repose angle tests. The scalping technique is thus validated for use in laboratory piles tests. The predictive capability of the calibrated model is further supported by strong agreement with additional experimental data. This calibrated and validated numerical DEM model can now be confidently applied to analyze the mechanical behavior of WR-based infrastructures across varying particle sizes and field conditions. Its application to simulate the natural mixing between dumped WR and uncemented paste backfill is presented in Part II of this companion study.

1. Introduction

Mining operations generate substantial volumes of mine wastes, primarily in the form of tailings and waste rock. Traditionally, these materials are stored on the surface in tailings storage facilities and waste rock piles. These surface storage methods have significant environment footprint. Chemically reactive mine waste can lead to acid mine drainage or contaminated neutral drainage. More critically, failures of tailings storage facilities can result in catastrophic tailings flood, which may destroy infrastructures and cause fatalities or injuries along their

Peer review under responsibility of Editorial Board of of Deep Resources Engineering.
* Corresponding author.
E-mail addresses: yuyu.zhang@polymtl.ca (Y. Zhang), li.li@polymtl.ca (L. Li), serge.ouellet@agnicoeagle.com (S. Ouellet), Louis-Philippe.Gelinas@agnicoeagle.com (L.-P. Gélinas).

https://doi.org/10.1016/j.deepre.2025.100232
Received 9 June 2025; Received in revised form 19 October 2025; Accepted 13 November 2025
Available online 14 November 2025
2949-9305/© 2026 The Authors. Publishing services by Elsevier B.V. on behalf of KeAi Communications Co. Ltd. This is an open access article under the CC BY license (http://creativecommons.org/licenses/by/4.0/).

paths [1].

Underground mining operations that incorporate backfill composed of mine waste offers several advantages. Backfilling significantly reduces the volume of surface-stored waste, thereby lowering the environment footprint. It also mitigates the geochemical and geotechnical risks associated with surface storage. Furthermore, cemented backfill made from mine waste can enhance ore recovery, reduce dilution, improve ventilation efficiency, and strengthen ground stability [2]. For these reasons, backfilling has become an integral component of most modern underground mining operations worldwide.

Currently, three primary types of backfill are used in underground mines: hydraulic backfill, paste backfill, and rock fill [3,4]. A large body of literature focuses on the application of individual backfill type [5–39]. A limited number of studies have explored the mechanical blending of waste rock with cemented backfill [4,40-43] or the graded waste rock and tailings [44-46]. These methods typically require crushing, sieving, mechanical mixing, specialized equipment, considerable energy input, which increase operation costs to control waste rock size and ensure homogenous mixing.

In Canada, a widely adopted practice involves directly dumping waste rock generated underground into stopes being filled with cemented paste backfill. This approach significantly reduces the volume of waste rock transported to the surface, which is particularly beneficial for deep mining operations, as it lowers energy consumption, greenhouse gas emissions, and operational costs [47]. Additionally, if the waste rock mixes well with the cemented paste backfill, the resulting composite material may exhibit superior mechanical properties compared to the individual components [48-50], and may reduce binder consumption, thereby lowing backfill costs.

Despite these advantages, directly dumping waste rock into stopes can introduce risks. Poor or incomplete mixing with the cemented paste backfill may result in unstable fill masses that collapse during subsequent stope excavation, leading to ore dilution, ore loss, or other adverse outcomes. Therefore, a thorough understanding of the natural mixing behavior between dumped waste rock and paste backfill is essential.

Zhang and Li [51] were the first to investigate this natural mixing process through small-scale laboratory experiments. They simulated a mine stope using a box setup and employed a waste rock sample with a controlled particle size range to facilitate separation and quantify mixing. While their study provides initial insights, further research is needed to understand and quantify this behavior under field conditions.

Although large boxes with larger waste rock particles can be used in laboratory experiments, replicating field-scale mixing remains challenging due to space constrains and the large particles sizes typically found in situ, often several tens of centimeters [52-57]. Numerical modeling is therefore necessary to capture size effects related to stope dimensions and particle sizes. A robust numerical model must account for both the granular feature of waste rock and the fluid-like behavior of paste backfill. While discrete element method (DEM)-based models effectively simulate granular materials, they do not inherently account for fluid interactions.

Recently, Zhang and Li [51] incorporated buoyancy and drug forces into a DEM-based numerical code [58] to simulate the interaction between granular materials and paste backfill. This enhanced model, termed f-EDEM, was validated against analytical solutions and used to study the natural mixing behavior between steel balls and paste backfill. Its model's ability to simulate the mechanical behavior of granular materials was further confirmed by comparing its results to experimental data. To ensure stability and reliability in numerical results, sensitivity analyses of key parameters such as time step and particle size distribution are crucial and must be conducted on a case-by-case basis [59,60]. Zhang and Li [60] also emphasized minimizing the number of calibrated parameters. When possible, physical property parameters such as particles' density, Young's modulus, and Poisson's ratio as well as particle-to-particle's static friction coefficient and restitution coefficient should be directly measured. The particle-to-particle's rolling resistance coefficient, while physically meaningful and assumed to be dependent on the particle shape and size, is difficult to measure directly and must be calibrated.

This study employs the f-EDEM model [51] to simulate the natural mixing behavior between dumped waste rock and uncemented paste backfill. The measured yield stress and calibrated viscosity of the paste backfill were adopted from Zhang and Li [51], as the same paste backfill material is used. Likewise, the waste rock material parameters (density, Young's modulus, Poisson's ratio for waste rock particles as well as restitution coefficient and static friction coefficient for particles to-particles interactions) were also taken from Zhang and Li [60], given the material's consistency. The only parameter requiring calibration is the rolling resistance coefficient, assumed to vary with the maximum particle sizes (d_{max}) and shape of the waste rock particles.

Accordingly, this research consists of two main components:

- Part I (this paper): Calibration of the rolling resistance as a function of d_{max} using repose angle pile tests and numerical simulations.
- Part II (companion paper): Validation of the predictive capacity of the calibrated model in simulating natural mixing behavior between dumped waste rock and paste backfill.

To enable laboratory testing, oversized waste rock particles must be excluded. Four scaling-down techniques exist for sample preparation: scalping, parallel, replacement, and quadratic methods [52-54,61-65]. The quadratic technique produces a unique particle size distribution (PSD) curve for a selected d_{max}, independently on the source of original material. It is rarely used. The most commonly used method in geotechnical engineering is the parallel scaling down technique. However, Deiminiat et al. [54] showed that it has never been rigorously validated. The scalping and replacement down techniques were previously deemed invalid based on flawed methodology [61,66,67].

Deiminiat et al. [54] further demonstrated that it is impossible to obtain finer particles than those present in the original material without additional grinding or sourcing from other materials, making it unfeasible to creates parallel PSD curves without altering the original sample. The replacement method, which involves adjusting a scalped sample by replacing removed coarse material with finer particles, is complex and remains non-validated. Recently, Deiminiat and Li [52] established that the scalping scaling down technique is suitable for extrapolating the shear strength of large in situ particles and is more straightforward than the other methods.

In this study, the scalping-down technique was adopted to prepare waste rock samples with different d_{max} values, consistent with its use in other related studies.

This paper (Part I) presents repose angle pile tests conducted on scalped waste rock samples with varying d_{max} values. The experimental results (pile geometries and repose angles) were used to calibrate the rolling resistance coefficients in the numerical model. These coefficients are expected to vary as the value of d_{max}. A relationship between the calibrated rolling resistance coefficient and d_{max} could thus be developed. Once validated, this relationship could be applied to predict rolling resistance coefficients of untested samples.

2. Repose angle pile tests and numerical modeling

The waste rock used in the tests was sourced from a mine located at the northwest of Québec, Canada. The lithological characteristics of the waste rock are described in Mercier-Langevin et al. [68]. The scalping down technique was applied to obtain samples with varying d_{max}.

Fig. 1a shows photographs of the scalped waste rock samples with d_{max} values of 8.0, 5.0, 3.35, and 2.0 mm, and corresponding masses M_{wr} of 900, 700, 300, and 200 g, respectively. The PSD curves of the four scalped samples are presented in Fig. 1b.

Fig. 2 presents a schematic presentation (Fig. 2a) and a photograph (Fig. 2b) of the repose angle test conducted using the scalped waste rock

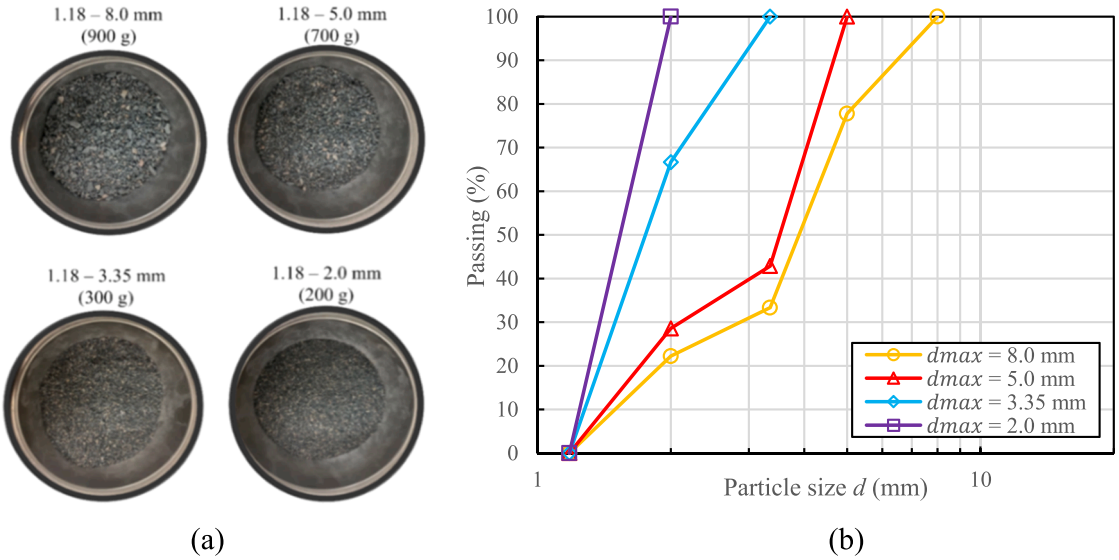

Fig. 1. Scalped waste rock samples with d_{max} values of 8.0, 5.0, 3.35, and 2.0 mm, respectively: (a) photographs of the samples; (b) PSD curves.

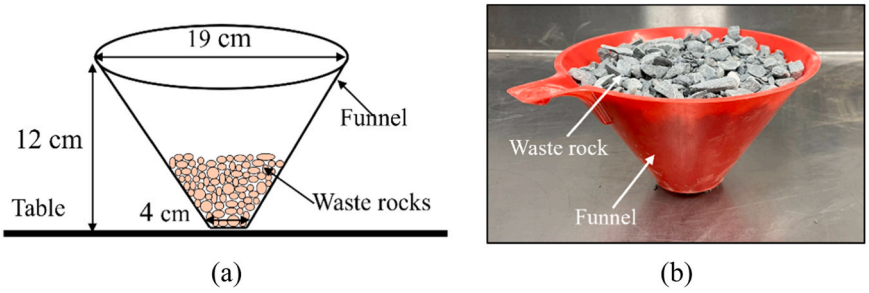

Fig. 2. Waste rock repose angle test: (a) a schematic presentation; (b) photograph of the funnel with a d_{max} of 8.0 mm waste rock.

sample with a d_{max} value of 8.0 mm and a mass of 900 g. The funnel used in the test had a top opening diameter of 19 cm, a base opening diameter of 4.0 cm, and an overall height of 12 cm. The test was performed by gently lifting the funnel at a rate of approximately 0.01 m/s until it was completely emptied.

Fig. 3 presents a side (Fig. 3a) and a top (Fig. 3b) view of the waste rock pile formed at the end of a repose angle test. The repose angle (θ) of the pile was calculated by measuring its height (H) and base diameter (D).

The test was conducted on waste rock samples with d_{max} values of 5.0, 3.35 and 2.0 mm, with corresponding masses of 700, 300, and 200 g, respectively. The measured repose angles (θ) for different d_{max} values are presented in Table 1. It can be seen that the repose angle increases with increasing d_{max}, from 2.0 to 8.0 mm, consistent with the findings reported by Deiminiat and Li [52]. These experimental results will be used in the numerical modeling with EDEM to calibrate the rolling resistance coefficient as a function of d_{max}.

Table 1
Measured repose angles (θ) of the four scalped waste rock samples.

Scalped waste rock sample	d_{max} (mm)	M_{wr} (g)	θ (°)
1	2.00	200	33.47
2	3.35	300	34.65
3	5.00	700	36.54
4	8.00	900	37.17

Table 2 presents the material parameters required for the EDEM model. The particle density of the tested waste rock was measured in our

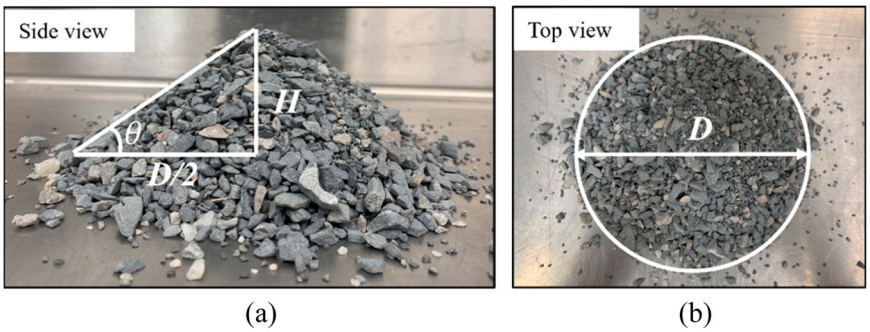

Fig. 3. Photographs of a waste rock pile formed with a sample with a d_{max} of 8.0 mm and a mass of 900 g.

Table 2
Model and material parameters necessary for EDEM model.

	Model and material parameters	Values	Determination
Particles of waste rocks	Density, ρ (kg/m^3)	2760	Measured
	Young's modulus, E (GPa)	46.8	Measured†
	Poisson's ratio, ν	0.19	Measured†
Particle to particle interaction	Restitution coefficient, μ_e	0.79	Measured‡
	Static friction coefficient, μ_s	0.466	Measured†
	Rolling resistance coefficient, μ_r	–	Unknown

Note: †by Major and Knupp [69]; ‡ by Sandeep et al. [70].

laboratory. The Poisson's ratio and static friction coefficient were adopted from Major and Knupp [69], who tested the same type of waste rock used in this study. The restitution coefficient was determined based on drop test results reported by Sandeep et al. [70]. The optimal value of Young's modulus was obtained by Zhang and Li [60]. The rolling resistance coefficient is the only unknown parameter and must be determined through calibration against experimental results.

Fig. 4 illustrates the numerical model built with EDEM for simulating the repose angle test for the waste rock with a d_{max} of 2.0 mm and a mass of 200 g. The physical model shown in Fig. 2a was reproduced in the simulation. Waste rock particles were generated in the funnel using EDEM's dynamic factory feature. The funnel was then lifted vertically at a speed of 0.01 m/s until it was completely emptied. The repose angle (θ) of the resulting waste rock pile was measured using EDEM protractor tool by clipping the pile at its center.

Before comparing numerical results with experimental data, it is essential to ensure that the numerical results are stable and reliable. As such, a sensitivity analysis of the time step must be conducted to determine the optimal value that guarantees numerical stability and reliability while minimizing computation time [60].

Fig. 5 illustrates the variation in the repose angle of the waste rock pile as a function of the time step using the parameters listed in Table 1 and a rolling resistance coefficient of 0.05. The results indicate that the repose angle stabilizes when the time step is equal to or less than 4.84×10^{-6} s. Therefore, this value is selected as the optimal time step for subsequent simulations.

As this time step, the numerically obtained repose angle is 22.49°, which is significantly lower than the experimentally measured value of 33.47°. To achieve better agreement between the experimental and numerical results, rolling resistance coefficient must be adjusted. Consequently, the entire numerical simulation process must be repeated for different values of the rolling resistance coefficient to identify the value that best replicates the experimental repose angle.

Fig. 6 illustrates the variation in the repose angle as a function of the rolling resistance coefficient, obtained from numerical modeling using the previously determined optimal numerical model. The experimentally measured repose angle of the waste rock pile is also included in the figure for comparison. The results show that a rolling resistance coefficient of 0.15 yields the best agreement between the simulated and measured repose angles. Therefore, the calibrated rolling resistance coefficient for the scalped waste rock sample with a d_{max} of 2.0 mm is determined to be 0.15.

The same calibration procedure was applied to scalped waste rock samples with d_{max} of 3.35 and 5.0 mm. Fig. 7 presents the variation in the calibrated rolling resistance coefficient as a function of d_{max}. Surprisingly, contrary to initial expectation, the rolling resistance coefficient does not exhibit significant variation as d_{max} increases from 2.0 to 5.0 mm. This observation suggests that the rolling resistance coefficient remains approximately constant, regardless of the d_{max} of scalped waste rock samples within this range. Based on this trend, a rolling resistance coefficient of 0.15 is predicted for the scalped waste rock sample with $d_{max} = 8$ mm. Numerical modeling using this predicted value yields a repose angle of 38.25°, which is in close agreement with the experimentally measured value of 37.17°.

Table 3 presents a summary of the repose angle measurements and the corresponding numerical results from the preliminary tests.

The good agreement between the measured repose angles and those obtained through numerical modeling indicates that the calibrated EDEM model is capable of reliably analyzing the geotechnical behavior of infrastructures composed of waste rock across a range of particle sizes and under varying conditions, including field-scale scenarios provided that sufficient computational resources are available.

However, the apparent contradiction between the nearly constant

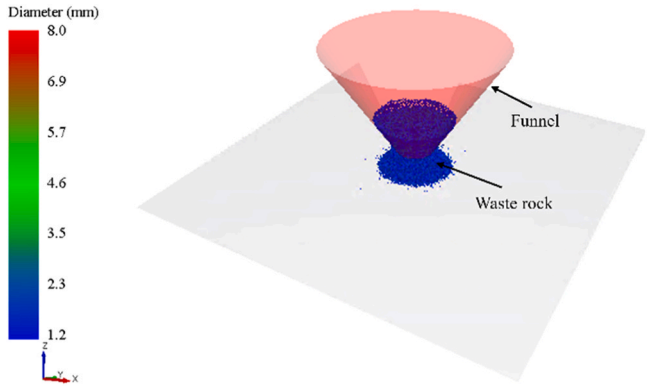

Fig. 4. Numerical model built with EDEM for simulating the repose angle test of waste rock with a d_{max} of 2.0 mm and a mass of 200 g.

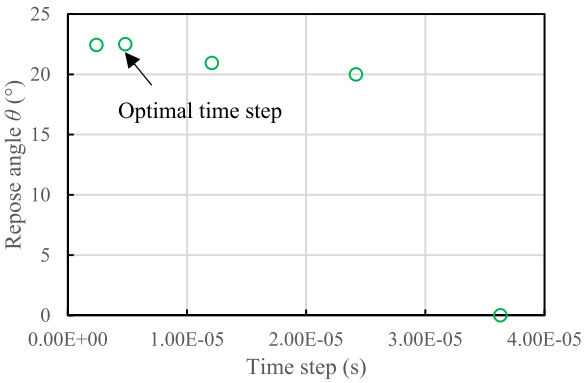

Fig. 5. Variation in the repose angle as a function of the time step, obtained by numerical simulations with the parameters listed in Table 1 and a rolling resistance coefficient of 0.05.

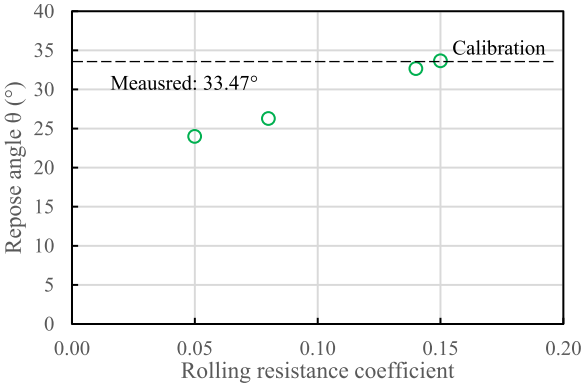

Fig. 6. Variation of repose angle as a function of rolling resistance coefficient, obtained from numerical simulations with optimal numerical models for the scalped waste rock sample with a d_{max} of 2.0 mm and a mass of 200 g.

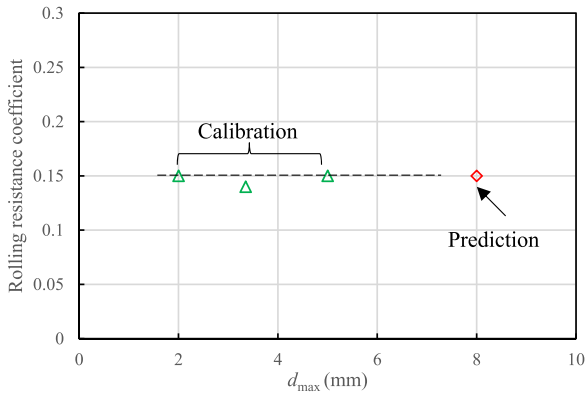

Fig. 7. Variation of the calibrated rolling resistance coefficient as a function of d_{max}.

Table 3
Experimentally measured and numerically reproduced repose angles (θ) for the four scalped waste rock samples.

Waste rock sample	d_{max} (mm)	M_{wr} (g)	Rolling resistance coefficient, μ_r		Repose angle, θ (°)	
			Value	How	Measured	Numerical
1	2.0	200	0.15	Calibration	33.47	33.64
2	3.35	300	0.14	Calibration	34.65	34.37
3	5.0	700	0.15	Calibration	36.54	36.87
4	8.0	900	0.15	Prediction	37.17	38.25

calibrated rolling resistance coefficient and the observed increase in measured repose angle as d_{max} increases from 2 to 8 mm warrants further investigation.

3. Additional laboratory tests and numerical modeling

The repose angle and the rolling resistance coefficient are two intrinsic properties of granular materials and, for a given material, are generally expected to exhibit consistent trends. Based on the measured repose angles of the scalped waste rock samples shown in Table 1, it was anticipated that the calibrated rolling resistance coefficients would also vary with changes in the d_{max}. However, as shown in Table 3, this was not the case: the calibrated rolling resistance coefficients remained nearly constant and appeared to be independent of d_{max}.

This apparent contradiction raises an important question: How can the divergence between the increasing measured repose angles and the constant numerically calibrated rolling resistance coefficient be explained? Should the discrepancy be attributed to limitation in numerical modeling, the experimental testing, or possibly both? A definitive answer cannot be reached if the reliability of either dataset is uncertain.

However, we have a high degree of confidence in the numerical model and its outputs. The model has been validated, and its applicability to simulate the mechanical behavior of granular materials has been demonstrated in previous studies [51,60]. Furthermore, the numerical simulations used to reproduce the measured repose angles of the scalped waste rock samples have been shown to be stable and reliable (Figs. 4 and 5). This leads us to scrutinize the experimental measurements more closely.

A review of Table 1 reveals that the measured repose angle increases not only with increasing values of d_{max} but also with the mass of waste rock used in the tests. Indeed, if a very small mass of waste rock is placed at the base of the funnel, the resulting pile will have a repose angle close to zero, suggesting that the measured repose angle is influenced by the mass of material used in the test.

In the experiments summarized in Table 1, the mass of waste rocks used for each pile test was determined arbitrarily. Therefore, it remains unclear whether the chosen masses were sufficient to ensure stable and reliable repose angle measurements. To investigate this, a sensitivity analysis was conducted to evaluate the effect of waste rock mass on the measured repose angle for four scalped waste rock samples with different values of d_{max}.

Fig. 8 presents the variation of repose angle θ as a function of waste rock mass (M_{wr}), using a funnel with a 4.0 cm base opening. The results show a consistent trend: for all four scalped waste rock samples, the measured repose angle increases as the mass of the waste rock increases from 50 to 900 g. Beyond 900 g, the repose angle stabilizes and remains effectively constant with further increases in mass.

These findings help to explain the previously observed increase in repose angle with increasing d_{max} in Table 1. Specifically, the masses used for the tests with d_{max} = 2, 3.35, and 5 mm were below the threshold of 900 g, meaning the resulting repose angle were likely underestimated and unreliable. When the used mass is smaller than the minimum required to form a stable pile, the measured repose angle cannot be considered representative of the material's intrinsic properties.

Another factor that can influence the measured repose angle is the opening diameter at the base of the funnel, denoted as W. Fig. 9 presents four funnels with base opening diameters W of 60, 40, 30 and 10 mm, respectively.

Fig. 10 shows the variation of the measured repose angle θ as a function of W/d_{max} ratio, obtained by using the four different funnels on a waste rock sample with a fixed d_{max} = 8.0 mm. It is important to emphasize that the variation in the W/d_{max} ratio arises solely from changes in W, not from change in d_{max} or from simultaneous variation of both parameters [53,71].

When the repose angle tests were conducted using the smallest funnel, with a base diameter of 10 mm (W/d_{max} = 1.25), the measured repose angle was zero. This is because all waste rock particles became lodged in the funnel, thereby preventing pile formation. As the W/d_{max} ratio increased, the measured repose angle also increased, stabilizing once the ratio exceeded 3.75.

These results demonstrate that the base diameter of the funnel significantly influences the stability and reliability of repose angle measurements. However, it is important to note that all previously presented pile tests were conducted using a funnel with a 40 mm base diameter. As a result, the corresponding W/d_{max} ratios in those tests were greater than 3.75, ensuring that the influence of funnel diameter was effectively eliminated.

Recognizing that stable and reliable repose angle measurement require the use of a funnel with a sufficiently large base diameter and an adequate quantity of material, all repose angle tests were repeated for

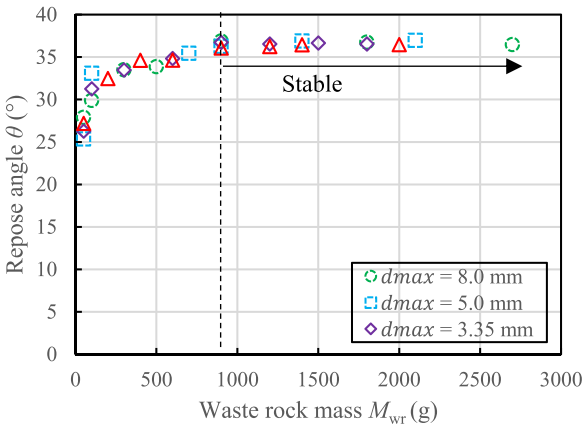

Fig. 8. Variation of repose angle θ as a function of waste rock mass M_{wr} for scalped waste rock samples with varying d_{max}, obtained by using a funnel with a 4.0 cm base opening.

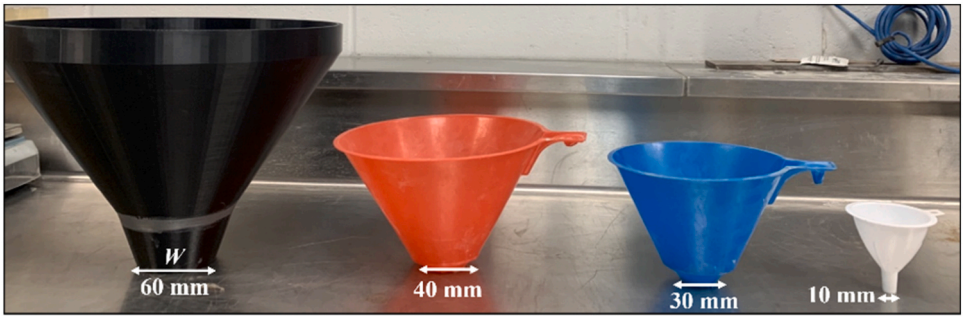

Fig. 9. Four funnels with different base opening diameters W for the repose angle tests.

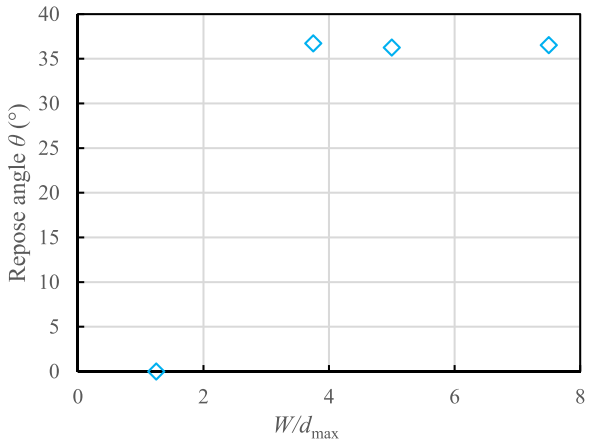

Fig. 10. Variation of the measured repose angle of the waste rock sample with a d_{max} of 8 mm as a function of the W/d_{max} ratio, obtained by using four funnels with different base diameters.

the four scalped waste rock samples using a funnel with base diameter of 40 mm. The masses of the waste rock samples with d_{max} of 2.0, 3.35, 5.0, and 8.0 mm were set to 1000, 1500, 3500, and 4500 g, respectively. These values were chosen to satisfy both the minimum required mass of 900 g and the minimum required W/d_{max} ratio of 3.75.

Fig. 11 shows the variation of the measured repose angle θ as a function of d_{max}, obtained from these revised experiments. The results show that the repose angle θ does not vary significantly as d_{max} increases from 2 to 8 mm. This trend aligns with the behavior observed in the numerically calibrated and predicted rolling resistance coefficients, thereby reinforcing the consistency between the experimental and numerical finings.

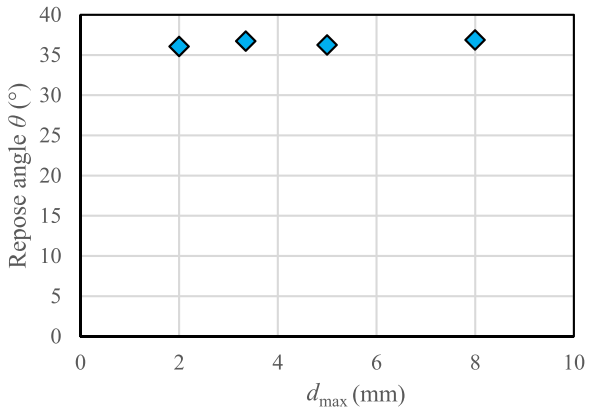

Fig. 11. Variation of the measured repose angle θ as a function of d_{max}, obtained from repose angle tests by respecting the minimum required mass of 900 g and the minimum required W/d_{max} ratio of 3.75.

Fig. 12 presents the numerical models to predict the experimental results shown in Fig. 11. The materials parameters used in the simulation are listed in Table 1, along with the calibrated and predicted rolling resistance coefficient of 0.15. All simulations were conducted using the previously determined optimal time step of 4.84×10^{-6} s.

The comparison between the numerical prediction and the new experimental results obtained under conditions that meet the minimum required mass and W/d_{max} ratio is shown in Fig. 13. The strong agreement between the numerical and experimental results further confirms the validity and robustness of the calibrated numerical model, specifically the EDEM code incorporating a rolling resistance coefficient of 0.15.

This validated EDEM model can therefore be confidently applied to analyze the geotechnical behavior of infrastructures composed of any sizes of waste rock across a range of particle sizes and under both laboratory and field conditions. It is particularly suitable for simulating complex processes such as the natural mixing behavior of dumped waste rocks and paste backfill within underground mine stopes.

4. Further validation of the calibrated numerical model

To further assess the validity of the calibrated numerical model presented in Section 3, additional simulations were performed to reproduce the repose angle test results of the waste rock sample with a $d_{max} = 2.0$ mm under varying sample masses. Specifically, numerical prediction were conducted for waste rock masses of 200, 400, 600, 900, and 1200 g. Fig. 14 presents the corresponding numerical models to simulate these conditions and predict the associated repose angles.

Fig. 15 presents the variation of repose angle as a function of sample mass, as obtained from both laboratory tests and numerical predictions using the calibrated numerical model. As expected, good agreement is obtained between the experimental data and the numerical results, further confirming the applicability and reliability of the calibrated model for analyzing the geotechnical behavior of waste rock materials across different conditions and particle sizes.

Moreover, both the experimental and numerical results indicate that the repose angle of scalped waste rock remains essentially unchanged with varying d_{max}. If this trend holds, it would suggest that the repose angle should consistently remain at with the range of approximately 36.2° to 36.8°, even as d_{max} increases from a few millimeters to values on the order of meters.

To examine the validity of this conclusion, as additional repose angle pile test was conducted using a scalped waste rock sample with a significantly larger $d_{max} = 70$ mm.

Fig. 16a shows a photograph of the scalped waste rock sample with a d_{max} of 70 mm. The corresponding PSD curve is presented in Fig. 16b, alongside the PDS curves of samples with d_{max} values of 8.0, 5.0, 3.35, and 2.0 mm for comparisons.

To perform the large-scale repose angle pile test, the 700 mm d_{max} waste rock sample was first placed into a cylindrical column with a

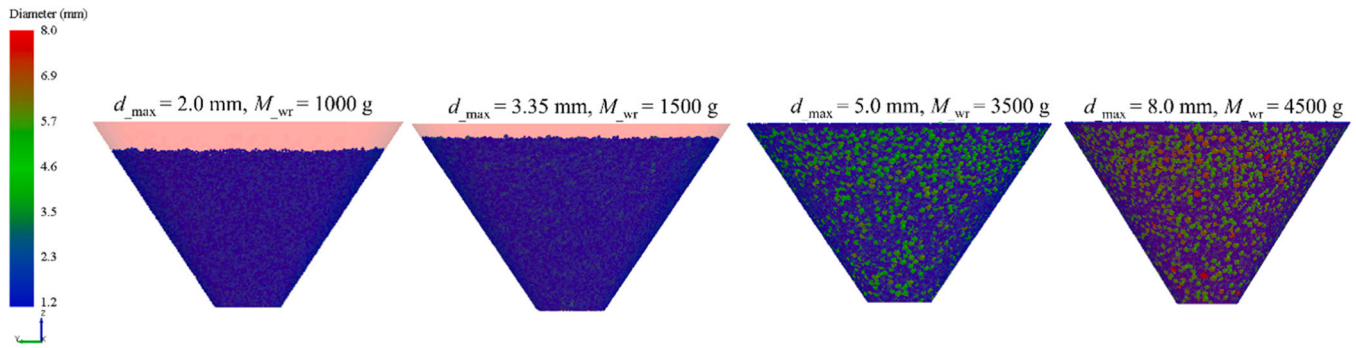

Fig. 12. Numerical models for predicting the experimental results presented in Fig. 11 (repose angle of waste rock with d_{max} of 2.0, 3.35, 5.0 mm and 8.0 mm, respectively).

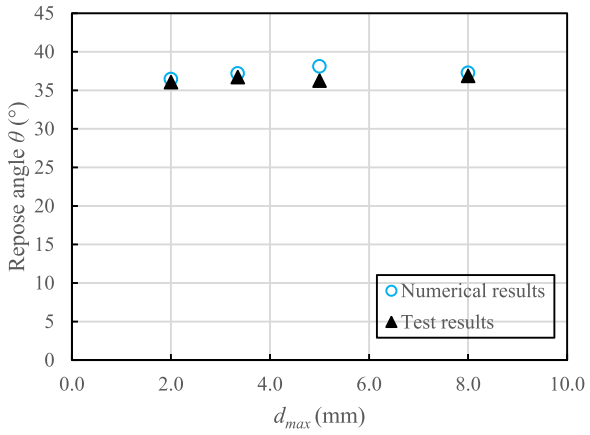

Fig. 13. Variation of repose angle as a function of d_{max}, obtained by laboratory tests and predicted by the calibrated numerical model (with the materials parameters presented in Table 1, optimal time step of 4.84 $\times 10^{-6}$ s and rolling resistance coefficient of 0.15).

height of 500 mm and a diameter of 300 mm (Fig. 17a). The test was initiated by carefully and gradually lifting the cylindrical column until it was completely emptied, allowing the material to form a conical pile under gravity.

Fig. 18 presents the variation of repose angle as a function of the waste rock mass for the scalped sample with a d_{max} = 70 mm. As observed in previous tests, the repose angle increases with increasing mass and eventually stabilizes at approximately 36.5°. This stabilized value aligns closely with those predicted by numerical modeling and with the extrapolated results from repose angle pile tests conducted on samples with d_{max} values ranging from 2.0 to 8.0 mm (Fig. 13). These findings further confirm the conclusion that, for scalped waste rock samples, the repose angle is essentially independent of d_{max}, provided that test conditions such as sample mass and W/d_{max} ratio are properly controlled.

5. Discussion

In this study, a series of repose angle pile tests were conducted using scalped waste rock samples with varying d_{max} to calibrate and validate a DEM-based numerical model. The initially measured repose angles (θ) appeared to increase with increasing d_{max}, a trend consistent with friction angles previously obtained from direct shear tests on similar scalped waste rock samples by Deiminiat and Li [52]. Based on this trend, a similar increase was initially expected for the rolling resistance coefficient (μ_r). However, calibration results revealed that μ_r remained nearly constant, showing low sensitivity to changes in d_{max}.

Since the numerical modeling was conducted rigorously and the results were deemed reliable, the experimental procedure for measuring repose angle was re-evaluated. Further investigation revealed that the initially observed trend of increasing θ with d_{max} was an artifact of insufficient sample mass. When the tests were repeated with sufficient mass and an appropriate W/d_{max} ratio, the measured repose angles stabilized and became nearly constant across all particle sizes, aligning well with the constant value of μ_r, obtained from numerical calibration. This resolved the contradiction between the experimental and numerical results.

However, this finding contrasts with the trend observed in the direct shear tests of Deiminiat and Li [52], where friction angles increased with d_{max} even under well-controlled conditions. A possible explanation lies in the distinction between static and dynamics repose angles: the direct shear test on waste rock samples in their loosest state likely corresponds to the static repose angle [71], while the pile tests in this study represent the dynamic repose angle. Future work is needed to gain a more comprehensive understanding of the relationship between static and dynamic repose angles for coarse granular materials. Moreover, Deiminiat and Li did not exclude fine particles, and the PSD curves of their scalped waste rock samples were significantly broader and more well-graded than those used in the current study. Additional research is required to determine whether the constant μ_r observed in this study is a special case, or whether it also applies more broadly, including the in situ waste rock.

Despite this uncertainty, the rolling resistance coefficient, being the only calibrated parameter in the numerical model, was found to be constant and independent of d_{max}. This reinforces the robustness and predictive capacity of the calibrated and validated model. As such, the

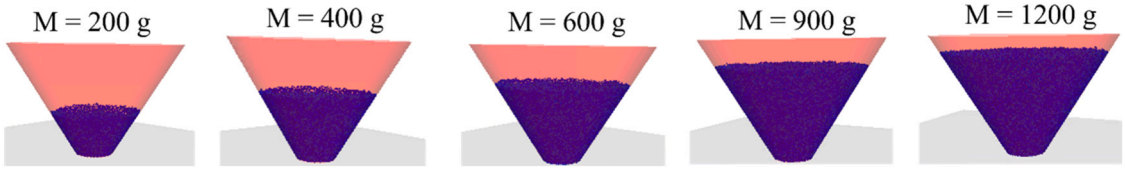

Fig. 14. Calibrated numerical models (with the materials parameters presented in Table 1, optimal time step of 4.84 $\times 10^{-6}$ s, and rolling resistance coefficient of 0.15) for predicting the repose angel test results of waste rock with a d_{max} of 2.0 mm and masses of 200, 400, 600, 900 and 1200 g, respectively.

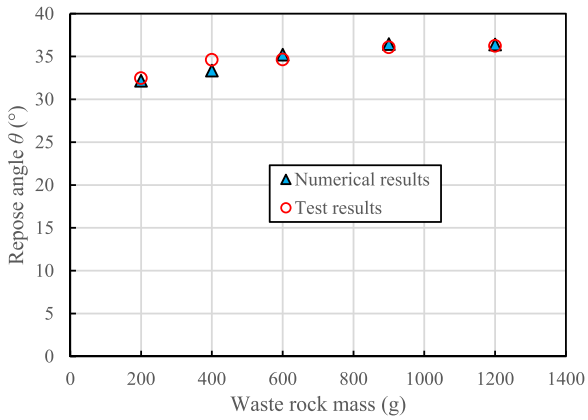

Fig. 15. The variation in the repose angle of the waste rock sample with a d_{max} of 2.0 mm as a function of mass, obtained from laboratory tests and numerical prediction using the calibrated numerical model (with the materials parameters listed in Table 1, an optimal time step of 4.84 $\times 10^{-6}$ s, and a rolling resistance coefficient of 0.15).

model can be confidently used to study the geotechnical behavior of infrastructures composed of waste rock materials of any size, including the nature mixing behavior between dumped waste rocks and paste backfill in underground mine stopes.

Additionally, the numerical and experimental results demonstrate that the scalping-down technique is an adequate method for excluding oversized particles from coarse granular materials, at least in the context of repose angle pile tests. This raises the question of whether numerical modeling is always necessary. For simple repose angle measurements, further experimental studies with a broader range of materials are

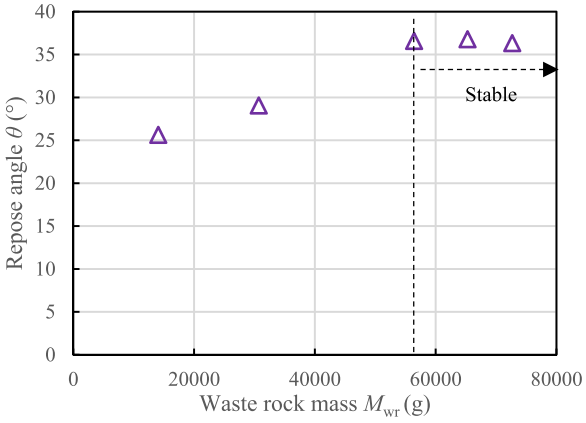

Fig. 18. Variation of the repose angle of waste rock as a function of mass, obtained by large-scale repose angle tests with waste rock d_{max} of 70 mm.

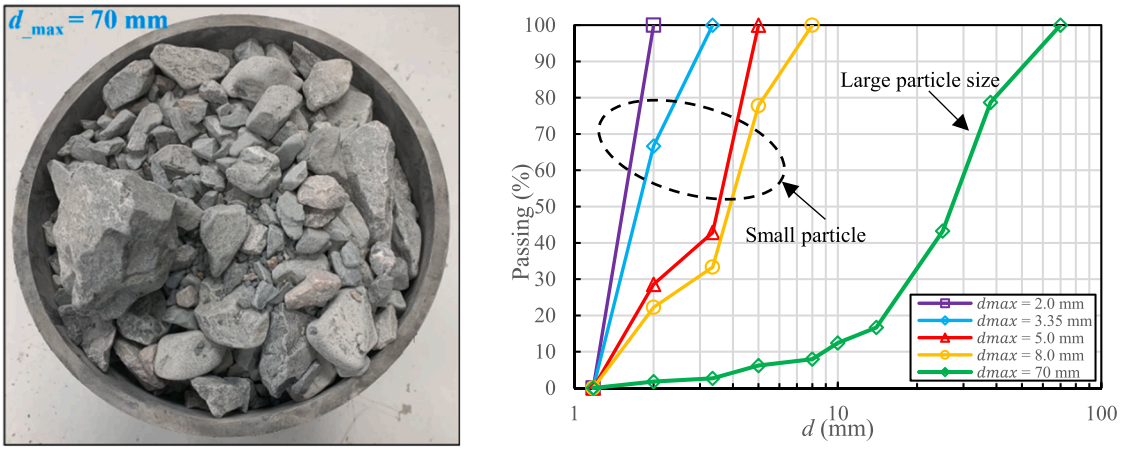

Fig. 16. Waste rock used in the large-scale repose angle pile test: (a) a photograph of the waste rock sample with a d_{max} of 70 mm; (b) PSD curves of the waste rock samples with different d_{max}.

Fig. 17. Large-scale repose angle test with the waste rock sample with a d_{max} of 70 mm: (a) a photograph of a cylindrical column filled with the waste rock sample; (b) a photograph of the large-scale waste rock pile.

needed to evaluate whether laboratory tests with scalped samples are sufficient. However, for more complex analyses, such as segregation, internal structure, of mixing behaviour in mine stopes, numerical modeling remains indispensable.

It is important to note that, in this study, the numerical repose angles were obtained from a single simulation run. Since DEM simulations generate the particles within a PSD between two neighboring sieves using a normal distribution function, the number and positions of generated particles can vary from one run to anther [60]. As a result, the outcomes may also differ slightly between runs. To improve the statistical reliability of numerical predictions, multiple simulations should be conducted for each test case. Furthermore, minor measurement errors can occur when estimating repose angles within EDEM code; therefore, multiple measurements are recommended to minimize this uncertainty.

Finally, a key limitation of the current numerical model lies in the simplification of representing non-spherical waste rock particles as spheres. While the effects of particle shape were partially accounted for through the calibrated rolling resistance coefficient, this approach is inherently approximate. Future work should explore the use of realistic shapes to improve model fidelity. Although this would reduce the number of calibrated parameters and better reflect the true mechanical behaviour of the material, it would also significantly increase computational time and resource requirements due to the complexity of contact calculations between irregularly shaped particles. Advanced computing technologies, such as high-performance GPUs, will be essential for enabling such simulations.

6. Conclusions

A series of repose angle pile tests were conducted on waste rock samples prepared using the scalping-down technique. The experimental results were used to calibrate the rolling resistance coefficient (μ_r) for samples with different d_{max}. An initial contradiction emerged between the trend of the measured repose angles and that of the calibrated rolling resistance coefficients. Further analyses led to the following key findings:

(1) Sensitivity of repose angle tests: The measured repose angle is influenced by both the mass of the waste rocks and the base opening diameter of the funnel. Stable and reliable measurements can only be obtained when the sample mass and funnel opening are sufficiently large. Sensitivity analyses are therefore essential to ensure stability and reliability of experimental results.
(2) Independence from d_{max}: Both the measured repose angle and the calibrated rolling resistance coefficient were found to be nearly constant, regardless of variation in d_{max} for scalped waste rock samples. This confirms that the repose angle of full-scale waste rock piles can be reliably determined through laboratory testing of appropriately prepared scalped samples.
(3) Validation of scalping-down technique: The results reaffirm the validity of the scalping-down technique for preparing coarse waste rock samples, at least in the context of repose angle pile testing.
(4) Predictive capacity of the numerical model: The good agreement between measured and numerically predicted repose angles confirms that the calibrated and validated DEM-based numerical model can be used to simulate the geotechnical behavior of waste rock materials across a wide range of particle sizes and infrastructure scales. This includes complex scenarios such as the mixing behavior of dumped waste rock and paste backfill in underground mine stopes, provided that adequate computing resources are available.

CRediT authorship contribution statement

Yuyu Zhang: Writing – original draft, Visualization, Validation, Software, Methodology, Investigation, Formal analysis, Data curation, Conceptualization. **Li Li:** Writing – review & editing, Supervision, Project administration, Methodology, Funding acquisition. **Serge Ouellet:** Writing – review & editing, Resources, Investigation, Formal analysis. **Louis-Philippe Gélinas:** Writing – review & editing, Resources, Formal analysis.

Declaration of Competing Interest

The authors declare that they have no known competing financial interests or personal relationships that could have appeared to influence the work reported in this paper. The author Li Li is a member of the editorial board for Deep Resources Engineering and was not involved in the editorial review or the decision to publish this article.

Acknowledgements

The authors acknowledge the financial support from the Natural Sciences and Engineering Research Council of Canada (NSERC RGPIN-2024–06859), Natural Sciences and Engineering Research Council of Canada (NSERC ALLRP 580767–22), and industrial partners of the Research Institute on Mines and the Environment (RIME UQAT–Polytechnique; http://rime-irme.ca). The anonymous reviewers are also gratefully acknowledged for their constructive comments and suggestions, which are very helpful for improving the quality and coherences of the manuscript.

References

[1] N.M. Rana, N. Ghahramani, S.G. Evans, et al., Catastrophic mass flows resulting from tailings impoundment failures, Eng. Geol. 292 (2021) 106262.
[2] P. Darling. SME Mining Engineering Handbook, third ed., Society for Mining, Metallurgy, and Exploration Inc, Littleton, Colorado, 2011.
[3] F. Hassani, J. Archibald, Mine backfill (CD-ROM), CIM, Montreal, QC, Canada, 1998.
[4] Y. Potvin, E. Thomas, A. Fourie, Handbook on mine fill. Australian Centre of Geomechanics, University of Western Australia, Nedlands, Australia, 2005.
[5] M. Aubertin, L. Li, S. Arnoldi, et al., Interaction between backfill and rock mass in narrow stopes, Soil Rock Am 1 (2) (2003) 1157–1164.
[6] J.B. Dalcé, L. Li, P.Y. Yang, Experimental study of uniaxial compressive strength (UCS) distribution of hydraulic backfill associated with segregation, Minerals 9 (3) (2019) 147.
[7] N. El Mkadmi, M. Aubertin, L. Li, Effect of drainage and sequential filling on the behavior of backfill in mine stopes, Can. Geotech. J. 51 (1) (2014) 1–15.
[8] E.M. Jaouhar, L. Li, Effect of drainage and consolidation on the pore water pressures and total stresses within backfilled stopes and on barricades, Adv. Civ. Eng. 2019 (1) (2019) 1802130.
[9] E.M. Jaouhar, L. Li, M. Aubertin, An analytical solution for estimating the stresses in vertical backfilled stopes based on a circular arc distribution, Geomech. Eng. 15 (3) (2018) 889–898.
[10] A.M.T. Keita, A. Jahanbakhshzadeh, L. Li, Numerical analysis of the stability of arched sill mats made of cemented backfill, Int. J. Rock Mech. Min. Sci. 140 (2021) 104667.
[11] A.M.T. Keita, A. Jahanbakhshzadeh, L. Li, Numerical analysis of the failure mechanisms of sill mats made of cemented backfill, Int. J. Geotech. Eng. 16 (7) (2022) 802–814.
[12] L. Li, Analytical solution for determining the required strength of a side-exposed mine backfill containing a plug, Can. Geotech. J. 51 (5) (2014) 508–519.
[13] L. Li, Generalized solution for mining backfill design, Int. J. Geomech. 14 (3) (2014) 04014006.
[14] L. Li, M. Aubertin, A modified solution to assess the required strength of exposed backfill in mine stopes, Can. Geotech. J. 49 (8) (2012) 994–1002.
[15] L. Li, M. Aubertin, An improved method to assess the required strength of cemented backfill in underground stopes with an open face, Int. J. Min. Sci. Technol. 24 (4) (2014) 549–558.
[16] L. Li, M. Aubertin, T. Belem, Formulation of a three-dimensional analytical solution to evaluate stresses in backfilled vertical narrow openings, Can. Geotech. J. 42 (6) (2005) 1705–1717.
[17] L. Li, M. Aubertin, R. Simon, et al., Modeling arching effects in narrow backfilled stopes with FLAC. Proceedings of 3rd international symposium on FLAC and FLAC3D numerical modelling in geomechanics. (2003) 211–219.
[18] G.S. Liu, L. Li, X.C. Yang, et al., Numerical analysis of stress distribution in backfilled stopes considering interfaces between the backfill and rock walls, Int. J. Geomech. 17 (2) (2017) 06016014.
[19] G.S. Liu, L. Li, X.C Yang, et al., Required strength estimation of a cemented backfill with the front wall exposed and back wall pressured, Int. J. Min. Miner. Eng. 9 (1) (2018) 1–20.

[20] G.S. Liu, L. Li, M.K. Yao, et al., An investigation of the uniaxial compressive strength of a cemented hydraulic backfill made of alluvial sand, Minerals 7 (1) (2017) 4.
[21] P. Pagé, L. Li, P.Y. Yang, et al., Numerical investigation of the stability of a base-exposed sill mat made of cemented backfill, Int. J. Rock Mech. Min. Sci. 114 (2019) 195–207.
[22] J.H. Qin, J. Zheng, L. Li, An analytical solution to estimate the settlement of tailings or backfill slurry by considering the sedimentation and consolidation, Int. J. Min. Sci. Technol. 31 (3) (2021) 463–471.
[23] J.H. Qin, J. Zheng, L. Li, Experimental study of the shrinkage behavior of cemented paste backfill, J. Rock Mech. Geotech. Eng. 13 (3) (2021) 545–554.
[24] M.A. Sobhi, L. Li, M. Aubertin, Numerical investigation of earth pressure coefficient along central line of backfilled stopes, Can. Geotech. J. 54 (1) (2017) 138–145.
[25] M.A. Sobhi, L. Li, Numerical investigation of the stresses in backfilled stopes overlying a sill mat, J. Rock Mech. Geotech. Eng. 9 (3) (2017) 490–501.
[26] R.F. Wang, F.T. Zeng, L. Li, Applicability of constitutive models to describing the compressibility of mining backfill: A comparative study, Processes 9 (12) (2021) 2139.
[27] R.F. Wang, F.T. Zeng, L. Li, Stability analyses of side-exposed backfill considering mine depth and extraction of adjacent stope, Int. J. Rock Mech. Min. Sci. 142 (2021) 104735.
[28] R.F. Wang, L. Li, Time-dependent stability analyses of side-exposed backfill considering creep of surrounding rock mass, Rock Mech. Rock Eng. 55 (4) (2022) 2255–2279.
[29] B.X. Yan, W.C. Zhu, C. Hou, et al., Characterization of early age behavior of cemented paste backfill through the magnitude and frequency spectrum of ultrasonic P-wave, Constr. Build. Mater. 249 (2020) 118733.
[30] B.X. Yan, H.W. Jia, E. Yilmaz, et al., Numerical investigation of creeping rockmass interaction with hardening and shrinking cemented paste backfill, Constr. Build. Mater. 340 (2022) 127639.
[31] B.X. Yan, H.W. Jia, E. Yilmaz, et al., Numerical study on microscale and macroscale strength behaviors of hardening cemented paste backfill, Constr. Build. Mater. 321 (2022) 126327.
[32] P.Y. Yang, L. Li, M. Aubertin, Theoretical and numerical analyses of earth pressure coefficient along the centreline of vertical openings with granular fills, Appl. Sci. 8 (10) (2018) 1721.
[33] P.Y. Yang, L. Li, M. Aubertin, et al., Stability analyses of waste rock barricades designed to retain paste backfill, Int. J. Geomech. 17 (3) (2017) 04016079.
[34] Y.L. Zhai, P.Y. Yang, L. Li, Analytical solutions for the design of shotcreted waste rock barricades to retain slurried paste backfill, Constr. Build. Mater. 307 (2021) 124626.
[35] J. Zheng, L. Li, Experimental study of the “short-term” pressures of uncemented paste backfill with different solid contents for barricade design, J. Clean. Prod. 275 (2020) 123068.
[36] J. Zheng, L. Li, Y.C. Li, Total and effective stresses in backfilled stopes during the fill placement on a pervious base for barricade design, Minerals 9 (1) (2019) 38.
[37] J. Zheng, L. Li, Y.C. Li, A solution to estimate the total and effective stresses in backfilled stopes with an impervious base during the filling operation of cohesionless backfill, Int. J. Numer. Anal. Methods Geomech. 44 (11) (2020) 1570–1586.
[38] J. Zheng, L. Li, Y.C. Li, Solutions to estimate the excess PWP, settlement and volume of draining water after slurry deposition. Part I: Impervious base, Environ. Earth Sci. 79 (2020) 124.
[39] J. Zheng, L. Li, Y.C. Li, Solutions to estimate the excess PWP, settlement and volume of draining water after slurry deposition. Part II: Pervious base, Environ. Earth Sci. 79 (2020) 275.
[40] G. Baldwin, A. Grice, Engineering the new Olympic Dam backfill system, Proc. Mass. (2000) 705–711.
[41] K. Kugan, S. Ian, A non-segregating Rocky Paste Fill (RPF) produced by co- disposal of cemented de-slimed tailings slurry and graded rockfill, Soc. Min. Metall. Explor. (2001).
[42] C. Lee, P. Gillot, Case study – a high strength paste aggregate backfill at Randgold’s Loulo mine in Mali. Mine Fill 2014, Proceedings of the Eleventh International Symposium on Mining with Backfill. Perth, Australia (2014) 231–242.
[43] W. Sun, H.J. Wang, K.P. Hou, Control of waste rock-tailings paste backfill for active mining subsidence areas, J. Clean. Prod. 171 (2018) 567–579.
[44] B.E. Wickland, G.W. Wilson, Self-weight consolidation of mixtures of mine waste rock and tailings, Can. Geotech. J. 42 (2) (2005) 327–339.
[45] G. Wilson, Co-disposal of tailings and waste rock, Geotech. N. 19 (2) (2001) 44–49.
[46] G.W. Wilson, B. Wickland, J. Miskolczi. Design and performance of paste rock systems for improved mine waste management. Rock Dumps 2008: Proceedings of the First International Seminar on the Management of Rock Dumps, Stockpiles and Heap Leach Pads, Australian Centre for Geomechanics, Perth, 2008, pp. 107–116.
[47] C. Lee, F.Q. Gu. An examination of improvements in co-disposal of waste rock with backfill, Beijing, 2017, pp. 338–345.
[48] I. Hane, T. Belem, M. Benzaazoua, et al., Laboratory characterization of cemented tailings paste containing crushed waste rocks for improved compressive strength development, Geotech. Geol. Eng. 35 (2) (2017) 645–662.
[49] H.F. Qiu, F.S. Zhang, L. Liu, et al., Influencing factors on strength of waste rock tailing cemented backfill, Geofluids 2020 (2020) 8847623.
[50] H.F. Qiu, F.S. Zhang, W.B. Sun, et al., Experimental study on strength and permeability characteristics of cemented rock-tailings backfill, Front. Earth Sci. 10 (2022) 802818.
[51] Y.Y. Zhang, L. Li, Experimental study on the natural mixing behaviour of waste rocks poured in a paste backfill, Int. J. Min. Reclam. Environ. 37 (10) (2023) 953–977.
[52] A. Deiminiat, L. Li, Experimental study on the reliability of scaling down techniques used in direct shear tests to determine the shear strength of rockfill and waste rocks, CivilEng 3 (1) (2022) 35–50.
[53] A. Deiminiat, L. Li, F.T. Zeng, Experimental study on the minimum required specimen width to maximum particle size ratio in direct shear tests, CivilEng 3 (1) (2022) 66–84.
[54] A. Deiminiat, L. Li, F.T. Zeng, et al., Determination of the shear strength of rockfill from small-scale laboratory shear tests: A critical review, Adv. Civ. Eng. 2020 (1) (2020) 8890237.
[55] M. James, M. Aubertin, B. Bussière, On the use of waste rock inclusions to improve the performance of tailings impoundments. 18th International Conference on Soil Mechanics and Geotechnical Engineering. Paris, France (2013) 735-738.
[56] V. Martin, M. Aubertin, G. Lessard, An assessment of hydrogeological properties of waste rock using infiltration tests and numerical simulations. 72nd Canadian Geotechnical Conference (GEO 2019). St. John’s, 2019.
[57] P.Y. Qiu, T. Pabst, Characterization of particle size segregation and heterogeneity along the slopes of a waste rock pile using image analysis, Environ. Earth Sci. 82 (23) (2023) 573.
[58] Altair EDEM, Altair EDEM 2022.2 Release Notes, Altair Engineering Inc, 2022.
[59] L. Li, Special issue on numerical modeling in civil and mining geotechnical engineering, Processes 10 (8) (2022) 1571.
[60] Y.Y. Zhang, L. Li, Optimization of discrete element method model to obtain stable and reliable numerical results of mechanical response of granular materials, Minerals 14 (8) (2024) 758.
[61] A. Hamidi, E. Azini, B. Masoudi, Impact of gradation on the shear strength-dilation behavior of well graded sand-gravel mixtures, Sci. Iran. 19 (3) (2012) 393–402.
[62] N. Marachi. Strength and deformation characteristics of rockfill materials, PhD Thesis, University of California, Berkeley, 1969.
[63] N.D. Marachi, C.K. Chan, H.B. Seed, Evaluation of properties of rockfill materials, J. Soil Mech. Found. Div. 98 (1) (1972) 95–114.
[64] C. Ovalle, S. Linero, C. Dano, et al., Data compilation from large drained compression triaxial tests on coarse crushable rockfill materials, J. Geotech. Geoenviron. Eng. 146 (9) (2020) 06020013.
[65] A. Varadarajan, K.G. Sharma, S.M. Abbas, et al., The role of nature of particles on the behaviour of rockfill materials, Soils Found 46 (5) (2006) 569–584.
[66] R.T. Donaghe, V.H. Torrey. Strength and deformation properties of earth-rock mixtures, Army Engineer Waterways Experiment Station, Vicksburg, MS, USA, 1985.
[67] S. Linero, C. Palma, R. Apablaza, R. Geotechnical characterisation of waste material in very high dumps with large scale triaxial testing. Proceedings of the 2007 International Symposium on Rock Slope Stability in Open Pit Mining and Civil Engineering. Perth, Australia (2007) 59-75.
[68] P. Mercier-Langevin, J. Goutier, B. Dubé, Precious- and base-metal deposits of the southern Abitibi greenstone belt, in: Superior Province, Ontario and Quebec. 14th Biennial Society for Geology Applied to Mineral Deposits Meeting Field Trip Guidebook, Geological Survey of Canada, Open File 8317, 2017, p. 86, 10.4095/306250.
[69] G. Major, R. Knupp, Report on feasibility-level pit slope design criteria Osisko Canadian Malartic project, Golder Associates Inc, 2008. ⟨https://archives.bape.gouv.qc.ca/sections/mandats/Mines_Malartic/documents/DA27.pdf⟩ (last access October 5, 2025).
[70] C.S. Sandeep, K. Senetakis, D. Cheung, et al., Experimental study on the coefficient of restitution of grain against block interfaces for natural and engineered materials, Can. Geotech. J. 58 (1) (2021) 35–48.
[71] A. Deiminiat, L. Li, A revision to the minimum required specimen width to the maximum particle size ratio of ASTM D3080/D3080M for direct shear test (DST) on coarse granular materials, ASTM Geotech. Test. J. (2025).

Dr. Li Li is a registered engineer with Ordre des ingénieurs du Québec (OIQ) and a professor of mining engineering at Polytechnique Montreal. He was the Head of Mining Engineering Program at Polytechnique Montreal between 2020 and 2023. He serves the Research Institute on Mines and Environment (RIME) UQAT-Polytechnique as a Scientific Director since May 2023 (https://irme.ca/en/rime/). He has more than twenty-year experience in geomechanical and geotechnical engineering. Over the past decade, his research has mainly focused on underground mining with backfill (stress estimation in backfilled stopes, sizing barricades made of waste rock, assessing required strength of backfill with side- or base- exposure).